RPE | Radiation Physics & Engineering
A Peer-Reviewed Journal
Published by K.N. Toosi University of Technology
http://rpe.kntu.ac.ir
Research Article

Radiation Physics and Engineering 2026; ?(?):?–?

Monte Carlo-based numerical assessment of metal and metal oxide nanoparticle parameters on cellular dose enhancement in proton therapy

Parisa Bidokhti[a], Keyhandokht Karimi-Shahri[a,*], Mahdi Ghorbani[b]

[a] *Department of Physics, Faculty of Science, University of Birjand, Birjand, Iran*
[b] *Biomedical Engineering and Medical Physics Department, School of Medicine, Shahid Beheshti University of Medical Sciences, Tehran, Iran*

HIGHLIGHTS

- Monte Carlo simulations assessed nanoparticle-induced dose enhancement in proton therapy at the cellular level.
- Dose enhancement increased linearly with nanoparticle concentration and decreased nonlinearly with size.
- Gold nanoparticles produced the highest dose enhancement compared to hafnium and iron oxides.
- The cytoplasm exhibited higher dose enhancement compared to the nucleus.
- Dose enhancement in proton therapy depends on nanoparticle material, size, and concentration.

ABSTRACT

Proton therapy is an effective cancer treatment due to its precise dose distribution and the presence of the Bragg peak. The incorporation of high-Z nanoparticles has emerged as a promising strategy to further enhance local dose deposition in tumor cells. This study aims to evaluate the dose enhancement effect of metal and metal oxide nanoparticles in cellular environments under proton irradiation. Monte Carlo simulations were performed using the GEANT4 toolkit with the GEANT4-DNA extension to model proton interactions at the microscopic scale. The influence of nanoparticle material (gold, iron oxide, and hafnium oxide), concentration (10-90 mg.ml^{-1}), and size (5-25 nm) on the dose enhancement ratio in the nucleus and cytoplasm of a single cell was investigated. Results show that the dose enhancement ratio (DER) increased linearly with nanoparticle concentration, while increasing nanoparticle size caused a nonlinear decrease in the DER. Among the studied nanoparticles, gold nanoparticles showed the highest dose enhancement due to their higher atomic number and density. Nanoparticle type, size, and concentration are critical factors for maximizing dose enhancement in proton therapy, with gold nanoparticles offering the greatest potential to increase therapeutic efficacy.

KEYWORDS

Proton therapy
Nanoparticle
Dose Enhancement Ratio
GEANT4 toolkit
Cell nucleus and cytoplasm

HISTORY

Received:
Revised:
Accepted:
Published:

1 Introduction

Cancer is a leading cause of global mortality, with projections indicating a sharp rise in incidence to 35 million annual cases by 2050, necessitating advanced therapeutic strategies (He et al., 2025). Among the emerging precision radiation modalities, proton beam therapy stands out for its ability to address this growing burden through superior tumor targeting and reduced toxicity.

Proton beam therapy represents a significant advancement in this regard. Its physical superiority over conventional photon therapy is due to the Bragg peak, which enables maximal dose deposition within the tumor while sparing surrounding healthy tissue (Mohan, 2022; Ramaekers et al., 2011; Alamgir et al., 2025). To further enhance tumor dose, high-atomic number (high-Z) nanoparticles are employed as radiosensitizers (Cunningham et al., 2021; Taheri et al., 2024; Rashid et al., 2025).

The combination of proton therapy with nanoparticle radio sensitization holds particular promise for improving therapeutic outcomes by amplifying local dose deposition through secondary electron production and reactive species generation. The efficacy of this approach depends critically on parameters such as nanoparticle material, concentration, and beam energy. Given the practical challenges of experimental proton beam studies, Monte Carlo simulation provides an essential virtual platform for their systematic investigation (Behrouzkia et al., 2019; Sah and

*Corresponding author: karimi.keyhandokht@gmail.com

https://doi.org/

Antosh, 2019).

Several key simulation studies have shaped this field. For instance, Sotiropoulos et al. (Sotiropoulos et al., 2017) employed the GEANT4 toolkit with the GEANT4-DNA extension to simulate a cellular model and calculate the direct proton damage with and without gold nanoparticles. Similarly, Rudek et al. (Rudek et al., 2019) used this extension to study gold nanoparticles in the cytoplasm under proton and carbon irradiation, reporting a maximum dose enhancement below 4%. In contrast, Peukert et al. (Peukert et al., 2020) observed a dramatically higher dose enhancement ratio (DER) exceeding 400% in their GEANT4 simulation, a result they attributed to their specific geometry and source definition. This stark discrepancy highlights a critical issue: methodological choices drastically influence outcomes. Studies vary widely in their fundamental approach- some model a single cell (Mohseni et al., 2020; Tabbakh, 2024), while others focus on a single nanoparticle (Kwon et al., 2016; Mansouri et al., 2024). Even within the latter category, the simulation setup differs, with primary particles emitted either from within the nanoparticle or from the surrounding medium. As noted by Taheri et al. (Taheri et al., 2023), all these methodological variations contribute significantly to the inconsistent results reported across the literature.

However, a critical review reveals considerable discrepancies in the reported DER values across studies, ranging from modest enhancements (<4%) to several hundred percent increases. These discrepancies are largely attributable to non-standardized and often incomparable simulation geometries, source definitions, and dose calculation methods (Peukert et al., 2020; Taheri et al., 2023). This lack of a consistent benchmark makes it difficult to draw definitive conclusions about nanoparticle efficacy. Moreover, although gold nanoparticles have dominated the literature, comparative studies on metal oxide nanoparticles (e.g., HfO_2 and Fe_2O_3) -which offer potential advantages in biocompatibility, cost-effectiveness, stability, and clinical translatability- remain scarce in the context of proton therapy, with very few dedicated investigations (Alamgir et al., 2024). Consequently, there is a clear need for a controlled, systematic investigation that directly compares these promising metal oxides with the gold (Au) under identical simulation conditions.

To address these methodological inconsistencies and the lack of comparative data for metal oxides, a controlled and systematic investigation was conducted. The GEANT4 toolkit was employed to directly compare the dose enhancement performance of conventional gold (Au) nanoparticles against two metal oxide nanoparticles - hafnium oxide (HfO_2) and iron oxide (Fe_2O_3)- under the same conditions. A more realistic cellular model was adopted, featuring nanoparticles uniformly distributed in the cytoplasm to better reflect biological uptake patterns observed in experimental studies. The DER for both the cell nucleus and the cytoplasm was evaluated separately across a range of proton beam energies (1, 5, 8, 10, and 15 MeV) and different therapeutic nanoparticle concentrations (10, 20, 30, 50, and 70 $mg.ml^{-1}$) with nanoparticle sizes (5, 10, 15, 20, and 25 nm). The primary novelty of this work lies in its head-to-head comparison, which aims to establish a clear benchmark and provide actionable insights for selecting the most effective nanoparticle type based on specific proton energy and concentration, thereby guiding future experimental designs and potential clinical translation.

2 Materials and Methods

2.1 Monte Carlo Simulation Tool

In this study, the Monte Carlo tool GEANT4 version 11 was used. The GEANT4 toolkit is a powerful and free tool for simulating particle tracking in materials, offering numerous capabilities, including the simulation of complex geometries, electric and magnetic fields, and nanoscale modeling (Allison et al., 2016). This code has been validated in numerous studies, particularly in radiobiology, medical physics, and dosimetry, and has become a reliable tool for simulations related to radiotherapy. To implement physical models at very low energies, the GEANT4-DNA extension was employed. GEANT4-DNA is a comprehensive extension of the GEANT4 toolkit, developed for radiobiological applications. Many studies have utilized this extension to calculate DNA damage and model DNA repair processes, as reported in published articles (Kyriakou et al., 2021; Carbone et al., 2025).

2.2 Cell and Nanoparticle Definition

The cell geometry was defined in a simplified manner, excluding DNA components, and consisted of two parts: the nucleus and the cytoplasm. According to (Rudek et al., 2019), a spherical cell with a diameter of 0.54 μm, made of water (1 $g.cm^{-3}$), was considered as the human cell nucleus, and a spherical shell with a thickness of 0.9 μm, also made of water, was defined as the cytoplasm surrounding the nucleus. Since the aim of this study is to calculate the DER resulting from the presence of various nanoparticles for proton sources, more complex geometries were not considered.

The nanoparticles were defined as spherical with diameters of 5, 10, 15, 20, and 25 nm and were randomly distributed within the cytoplasm volume. Several concentrations commonly used in clinical settings, including 10, 20, 50, 70, and 90 $mg.ml^{-1}$ for the nanoparticles, were considered, as frequently reported in many studies (Akhdar et al., 2022; Chen et al., 2020; Lin et al., 2015; Liu et al., 2015), since lower concentrations exhibit reduced biological effects. These five concentrations correspond to 0.1%, 0.2%, 0.5%, 0.7% and 0.9% by weight, respectively. Additionally, three different nanoparticle materials were considered: gold (19.3 $g.cm^{-3}$), hafnium oxide (9.68 $g.cm^{-3}$), and iron oxide (5.23 $g.cm^{-3}$). Gold nanoparticles are preferred due to their unique characteristics. Despite their relatively high cost, their high electron density, tunable size, ease of synthesis, low cytotoxicity, effective tumor-targeting capability, and chemical stability render them among the most promising metallic nanoparticles for biomedical applications (Cao et al., 2024; Shrestha et al.,

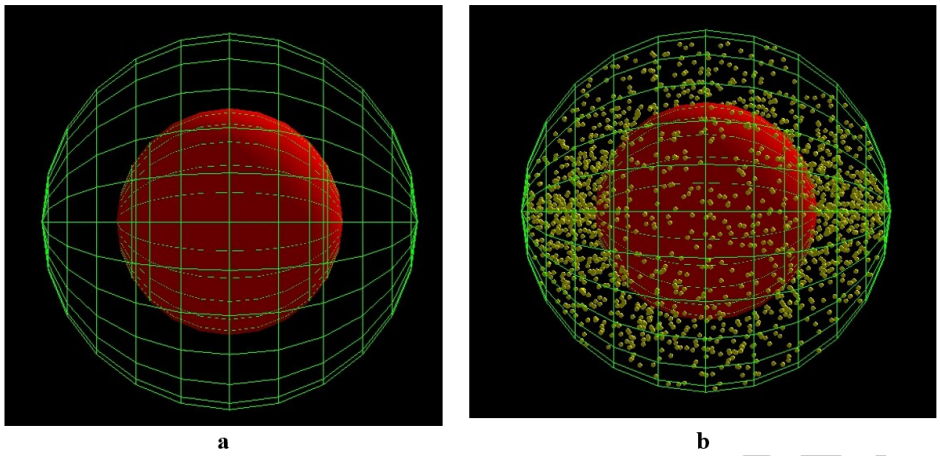

Figure 1: (a) View of the cell geometry in GEANT4. (b) View of the cell with nanoparticles incorporated into the cytoplasm.

2016). Hafnium oxide nanoparticles have also attracted increasing attention due to their stability, biocompatibility, and selective tumor uptake. For instance, Gerken et al. reported in vitro that these nanoparticles notably improve dose deposition and catalytic effects under photon and proton irradiation (Gerken et al., 2022). Finally, iron oxide was investigated in this study owing to its favorable biocompatibility, low cost, and widespread use in radiotherapy. Notably, Ma et al. demonstrated the enhanced radiobiological effects of magnetic nanoparticles on pancreatic cancer cells (BxPC3) within a combined proton therapy and hyperthermia framework (Ma et al., 2024). Their results showed that magnetic nanoparticles significantly increased radio sensitivity, leading to reduced cancer cell survival, elevated DNA damage, and increased production of cytotoxic reactive oxygen species (ROS), thereby markedly enhancing cancer cell mortality.

All nanoparticles were randomly distributed throughout the cytoplasm. To represent the case without nanoparticles, the nanoparticle material was considered as water to match the composition of the cytoplasm. Due to the different densities of the nanoparticles, the number of particles introduced into the cytoplasm varied for each desired concentration. Tables 1 to 3 present the number of each nanoparticle type, categorized by material, density, and concentration.

Figure 1 illustrates the cell geometry in GEANT4, where the red sphere represents the cell nucleus and the green shell represents the cytoplasm (a). In part (b) of the figure, the same cell is shown with the presence of nanoparticles (1000 particles), which were randomly distributed throughout the cytoplasm volume.

2.3 Radiation Source Definition

Monoenergetic proton beams with energies of 1, 5, 8, 10, and 15 MeV were defined as the radiation source. The beam was modelled as a circular surface source with a diameter equal to that of the cell (0.9 μm), emitted from the left toward the cellular model. Although a spread-out Bragg peak (SOBP) is used clinically for tumor treatment, monoenergetic protons were employed in this study since the target volume is a single small cell. The energy range was selected to cover the energies present within the SOBP region. In fact, within the SOBP, the proton energy spectrum ranges from a few keV up to several tens of MeV. In this study, the most probable energies within the SOBP, as reported by Martinez and colleagues (Martínez-Rovira and Prezado, 2015), were chosen. Therefore, these data can be reasonably used to support preclinical studies. The approach of selecting multiple monoenergetic protons instead of an SOBP has been validated in published studies (Rajabpour et al., 2022; Tabbakh, 2024). A total of 10 million protons were simulated, which reduced the statistical error to less than 0.1%.

2.4 Physics of the Problem

In this simulation, two physics lists were implemented simultaneously. One was the physics list known as DNA Physics, covering interactions within the cellular environment, and the other was the Livermore model, covering interactions within the nanoparticle environment. For defining DNA physics, the G4EmDNAPhysics_option2 class was used, which includes comprehensive microscopic and nanoscopic interactions for protons and secondary electrons. This data library is based on the track-structure algorithm and contains prebuilt physical models with appropriate cross sections for particle transport at low energies and at the nanometer scale. To define electron interactions, the following models were employed: G4DNABornExcitation for electronic excitation, G4DNAChampionElastic for elastic scattering, G4DNAMeltonAttachment for ionization, G4DNABornIonisation for molecular attachment, and G4DNASancheExcitation for vibrational excitation (Polopetrakis et al., 2025). The secondary particle production cutoff in the DNA physics model was set to 1 nm, indicating that all secondary particles with ranges shorter than 1 nm are not transported. The minimum energy considered in the G4EmDNAPhysics_option2 model was 7.4 eV, as energies below this threshold do not have sufficient ionization potential in water. Since the dose calculation in this study corresponds only to the physical stage, the

Table 1: Total number of Au nanoparticles simulated in the cellular model, categorized by material, diameter, and concentration.

Diameter (nm)	Number of NPs				
\Concentration ($mg.ml^{-1}$)	10	20	50	70	90
5	3019	6038	15094	21131	27168
10	378	755	1887	2642	3396
15	112	224	559	783	1007
20	48	95	236	331	425
25	25	49	121	170	218

Table 2: Total number of Fe_2O_3 nanoparticles simulated in the cellular model, categorized by material, diameter, and concentration.

Diameter (nm)	Number of NPs				
\Concentration ($mg.ml^{-1}$)	10	20	50	70	90
5	11216	22431	56077	78508	100939
10	1402	2804	7010	9814	12618
15	416	831	2077	2908	3739
20	176	351	877	1227	1578
25	90	180	449	629	808

Table 3: Total number of HfO_2 nanoparticles simulated in the cellular model, categorized by material, diameter, and concentration.

Diameter (nm)	Number of NPs				
\Concentration ($mg.ml^{-1}$)	10	20	50	70	90
5	6025	12050	30124	42174	54224
10	754	1507	3766	5272	6778
15	224	447	1116	1562	2009
20	95	189	471	659	848
25	49	97	241	338	434

pre-chemical and chemical stages were not simulated.

For defining the physics of interactions within the nanoparticles, the Livermore model based on the condensed-history algorithm was employed. Since DNA physics is not available for secondary photons, the same Livermore model was applied throughout the cell. The secondary particle production cutoff in the Livermore model was also set to 1 nm. Although new cross-section data, referred to as DNA physics, have been developed for gold at the nanometer scale (Polopetrakis et al., 2025), because one of the objectives of this study is to compare nanoparticles of different materials, identical physical conditions needed to be applied for all cases to ensure a reliable comparison. Therefore, the new cross-section data were not used, and the Livermore model was applied consistently for all cases. An innovation introduced in the physics modelling is the inclusion of hadronic models within the nanoparticles. Since heavy charged particles are involved, nuclear interactions between protons and the atomic nuclei of the nanoparticles are possible, which can lead to the emission of additional secondary particles. Therefore, in addition to standard electromagnetic physics, the QGSP_BIC base class was used as the reference physics. This physics class includes models for elastic and inelastic nuclear interactions (G4HadronPhysicsQGSP_BIC and G4HadronElasticPhysics), neutron interactions (G4NeutronTrackingCut), ion interactions (G4IonPhysics), stopping interactions (G4StoppingPhysics FritiofWithBinaryCascade), and decay processes (G4DecayPhysics) (Incerti et al., 2010). Decay physics is necessary to enable the emission of characteristic X-rays or Auger electrons following the excitation of target atoms.

2.5 Calculation of the DER

For all simulation cases, the DER was calculated using Eq. (1) (Tsiamas et al., 2013). This ratio is defined as the absorbed dose in the cytoplasm and nucleus in the presence of nanoparticles divided by the dose in the same volume with water nanoparticles.

$$DER = \frac{D_{NP}}{D_{WNP}} \tag{1}$$

In this equation, D_{NP} represents the absorbed dose in each target volume (nucleus or cytoplasm) in the presence of a nanoparticle made of any material other than water, while D_{WNP} denotes the dose in the same target volume when the nanoparticle is assumed to be made of water. For simulation validation, the data reported by Rudek et al. (Rudek et al., 2019) were used. In this validation setup, the cell was irradiated with 10 MeV protons, and a high nanoparticle concentration of 500 $mg.ml^{-1}$ (as reported in the reference) was applied. The DER values calculated in this study were subsequently compared with the reference results. All simulations were performed on a high-performance computing system equipped with 16 CPU threads and 32 GB of RAM.

Table 4: Comparison of DER for the cytoplasm and the cell nucleus induced by 10 MeV protons in this study and Rudek et al (Rudek et al., 2019).

Region	DER		Difference (%)
	Present study	Rudek et al.	
Nucleus	1.019	1.020	0.070%
Cytoplasm	1.035	1.034	0.100%

3 Results

3.1 Validation

Table 4 presents the DER values for both the cytoplasm and the nucleus. In this configuration, the gold nanoparticles were assumed to have a concentration of 500 mg.ml^{-1} and a diameter of 10 nm. The error bars represent a maximum statistical uncertainty of 1%. As shown in Table 4, there is an excellent agreement (maximum differences are about 0.1%) between the results obtained in this study and those reported by Rudek et al. (Rudek et al., 2019).

3.2 DER as a Function of Nanoparticle Concentration

Figures 2 and 3 present the DER values for proton beams at different energies in the presence of gold nanoparticles with a diameter of 5, 10, 15, 20, and 25 nm and concentrations of 10, 20, 50, 70, and 90 mg.ml^{-1} in the cytoplasm and the nucleus, respectively. In all these plots, the error

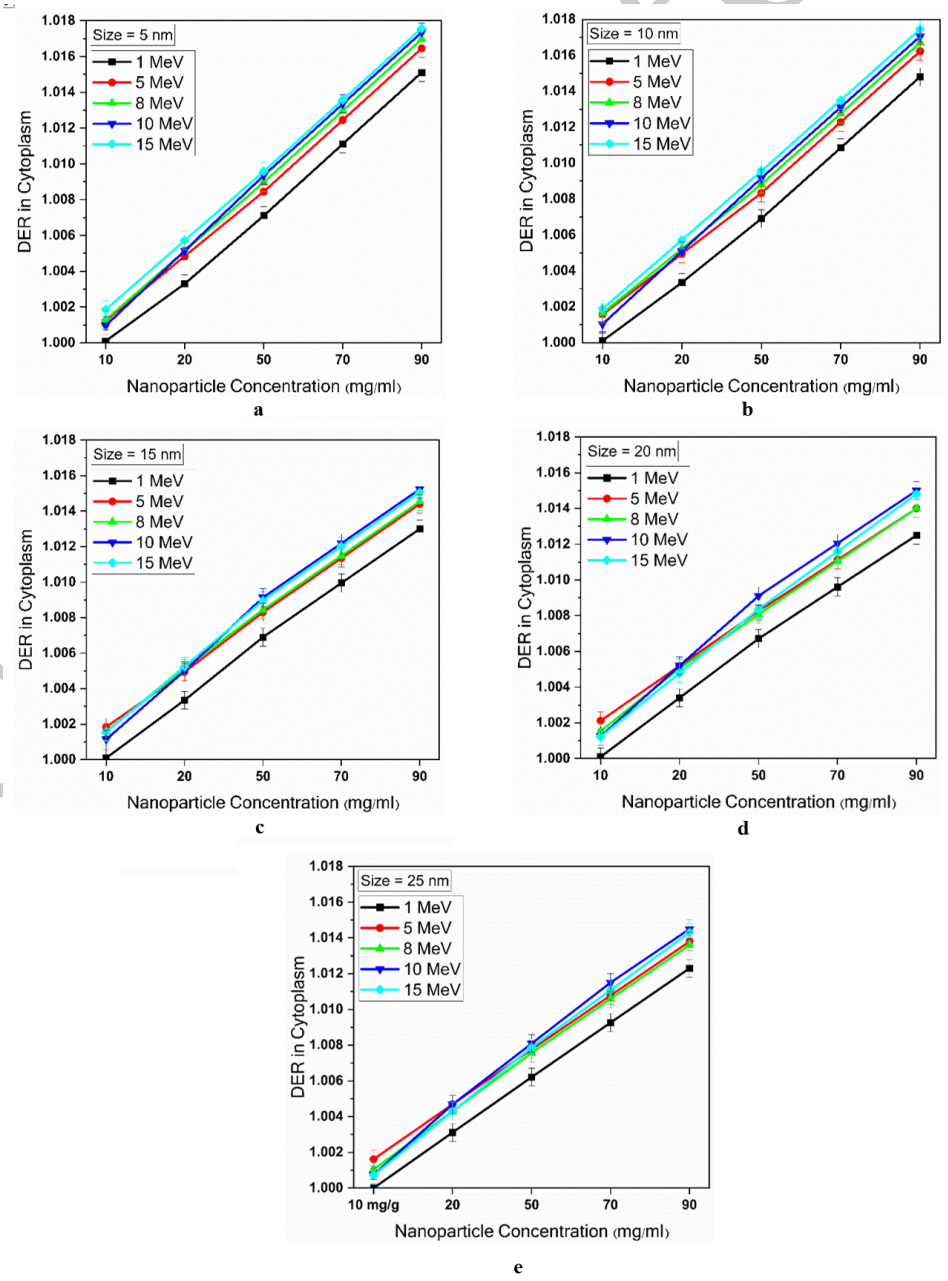

Figure 2: DER at different proton energies for 5, 10, 15, 20, and 25 nm gold nanoparticles at concentrations of 10, 20, 50, 70, and 90 mg.ml^{-1} in (a, b, c, d, e) the cytoplasm.

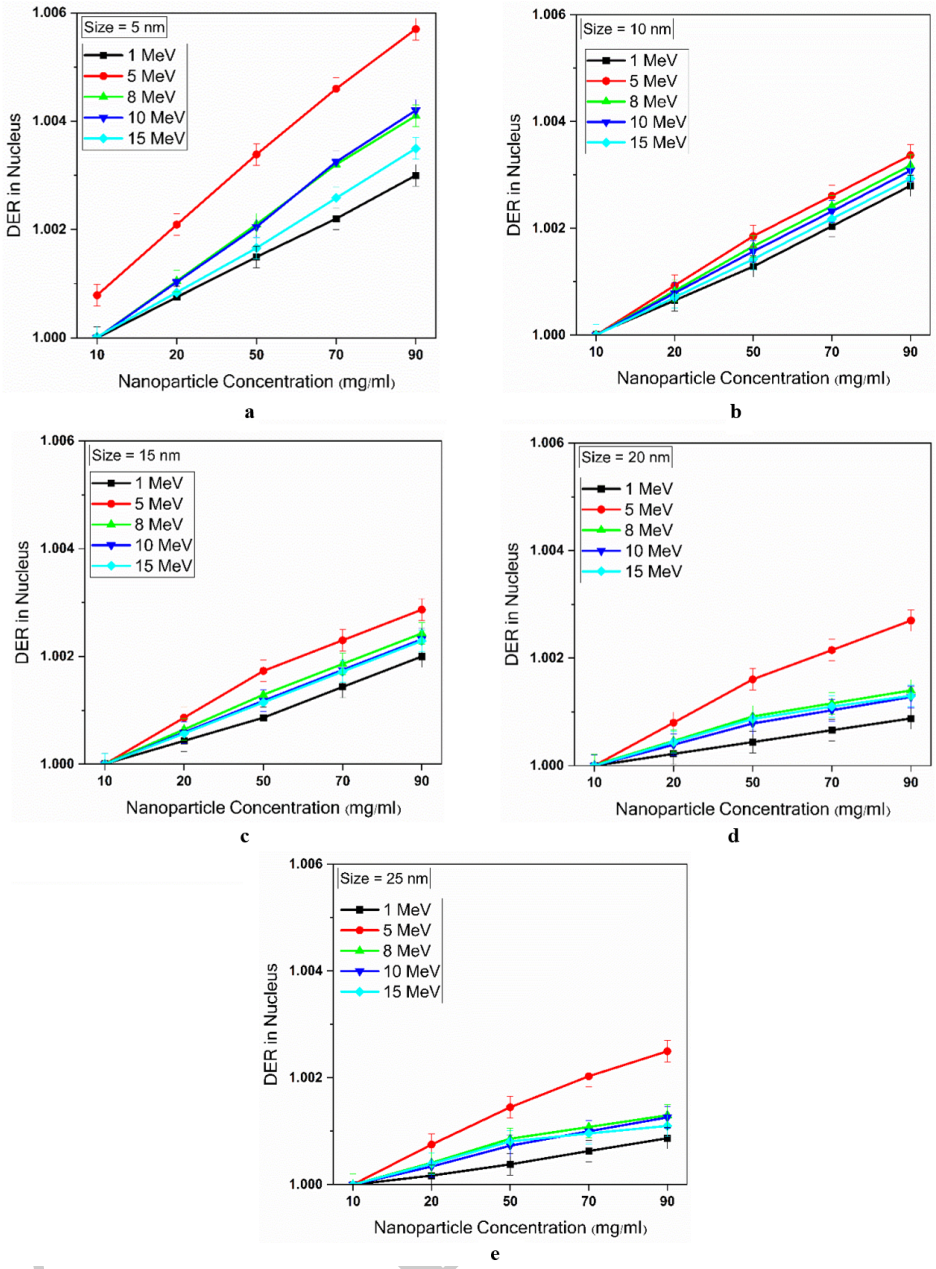

Figure 3: DER at different proton energies for 5, 10, 15, 20, and 25 nm gold nanoparticles at concentrations of 10, 20, 50, 70, and 90 mg.ml^{-1} in (a, b, c, d, e) the nucleus.

bars represent a maximum uncertainty of 0.05%.

Figures 2 and 3 illustrate that the DER increased with nanoparticle concentration in both the cytoplasm and the nucleus for all energies. In addition, the results reveal that the highest DER enhancement is observed in the cytoplasm at 15 MeV and in the nucleus at 5 MeV. This trend holds for all nanoparticle sizes investigated.

3.3 DER as a Function of Nanoparticle Size

To investigate the DER as a function of nanoparticle size, only a concentration of 90 mg.ml^{-1} was considered. Figure 3 shows the DER values for proton beams at different energies in the presence of gold nanoparticles at 90 mg.ml^{-1} with varying diameters of 5, 10, 15, 20, and 25 nm.

As shown in Fig. 4, the DER values depend on the nanoparticle size and decrease as the nanoparticle diameter increases.

3.4 DER as a Function of Nanoparticle Material

Gold nanoparticles, hafnium oxide, and iron oxide were compared. To investigate the effect of nanoparticle material on DER, only a concentration of 90 mg.ml^{-1} and a diameter of 5 nm were selected. This choice was made to allow a comparison of the maximum DER values. Figure 5 presents the results of this comparison for the energies investigated.

As the results show, gold has the maximum DER value at all energies and throughout the entire cell.

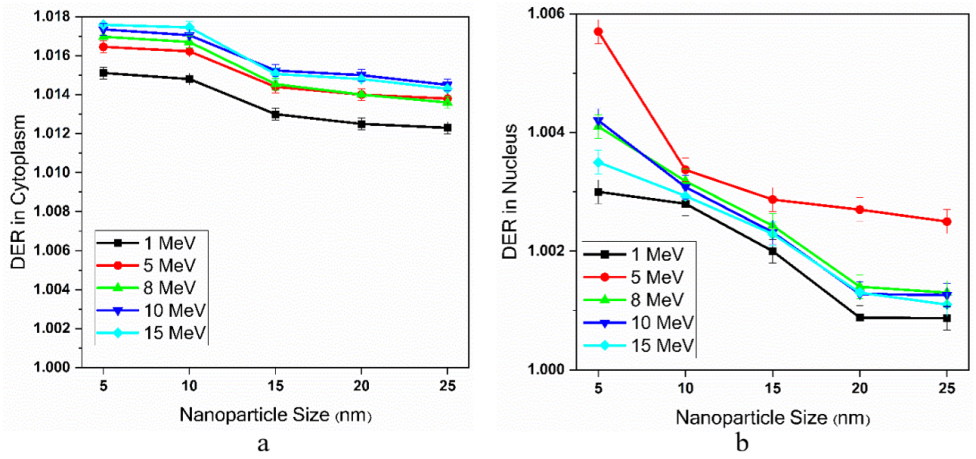

Figure 4: DER for gold nanoparticles at a concentration of 90 mg.ml^{-1} with different diameters at various proton energies in (a) the cytoplasm and (b) the nucleus.

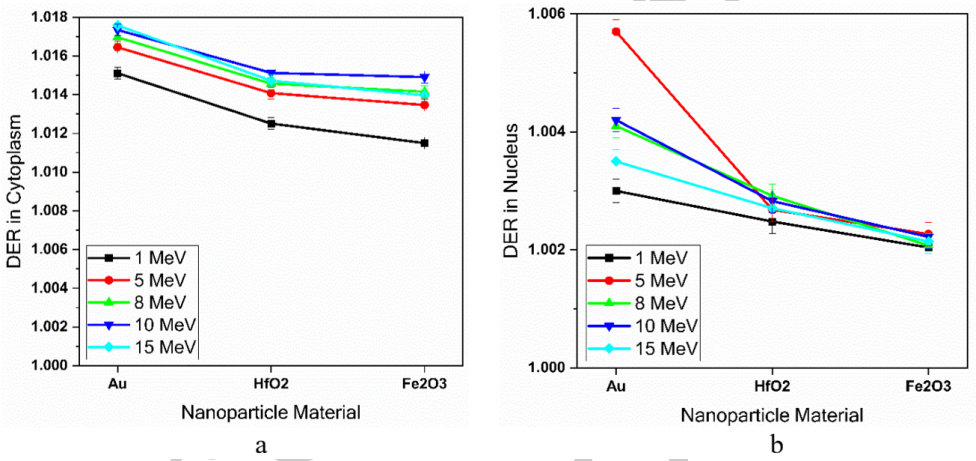

Figure 5: DERs for gold, hafnium oxide, and iron oxide nanoparticles at a concentration of 90 mg.ml^{-1} and a diameter of 5 nm at different proton energies in (a) the cytoplasm and (b) the nucleus.

4 Discussion

Several key parametric trends were elucidated. Regarding cellular compartments, the DER was consistently higher in the cytoplasm than in the nucleus, which directly reflecting the exclusive cytoplasmic localization of the nanoparticles in this model. This underscores the principle that dose enhancement is largely confined to the site of nanoparticle presence.

A clear dependence on nanoparticle concentration and size was observed, governed by distinct physical mechanisms. As shown in Figs. 2 and 3, the DER increased nearly linearly with nanoparticle concentration, in good agreement with prior studies (Rudek et al., 2019). This near-linear trend is a direct consequence of the proportional increase in the total mass and number of high-Z atoms within the irradiation volume at higher concentrations. A greater number of nanoparticles provides a correspondingly larger macroscopic cross-section for interaction with incident protons, leading to enhanced production of secondary electrons and increased local energy deposition. Conversely, as shown in Fig. 4, the DER exhibited a pronounced non-linear decrease with increasing nanoparticle diameter, with 5 nm emerging as a potentially optimal size. This inverse relationship stems from geometric and statistical factors at a fixed concentration (mass per unit volume). For a given concentration, the density of nanoparticles decreases cubically with increasing diameter. Fewer, more widely spaced nanoparticles result in a lower probability of a proton track intercepting a nanoparticle during its traversal through the cytoplasm. Consequently, despite the increased individual interaction probability of a single larger nanoparticle, the overall macroscopic interaction probability across the irradiated volume is reduced, leading to a lower dose enhancement. This observation aligns with findings by Peukert et al. (Peukert et al., 2020), highlighting the critical trade-off between nanoparticle size and density.

Based on the plots presented in Fig. 5, which compare DER values for proton beams in the presence of gold, hafnium oxide and iron oxide nanoparticles, it is evident that gold nanoparticles provide the greatest enhancement of cellular dose. The superior performance of gold compared to other metals can be attributed to its exceptionally high density and atomic number. Higher density and atomic number increase the probability of in-

teractions with primary particles, resulting in a higher deposited dose. Upon entering the target volume, protons undergo multiple scattering events, leading to the loss of part of their kinetic energy, with the mediums density and atomic number being key factor in proton slowing down. Therefore, nanoparticles with a high atomic number, such as gold, interact more strongly with incident protons and generate a large number of secondary electrons through atomic ionization. This leads to a significant reduction in proton energy as they traverse the nanoparticles, thereby increasing the dose delivered to the target region (Tabbakh, 2024). To further clarify the material-dependent interaction behavior of protons, Figure 6 presents the stopping power of protons in water, gold, hafnium oxide, and iron oxide as a function of proton energy. In proton therapy, unlike low-energy photon irradiation, where the photoelectric cross section exhibits a strong $Z^4 - Z^5$ dependence (Khan and Gibbons, 2014; Attix, 1986), proton energy loss in the MeV range is predominantly governed by Coulomb interactions with atomic electrons (electronic stopping), while nuclear interactions contribute to a lesser extent (Ziegler et al., 2010). The stopping power ($\mathrm{d}E/\mathrm{d}x$) represents the cumulative effect of these microscopic interaction cross sections and therefore provides a physically meaningful basis for comparing different materials in terms of energy transfer efficiency (Attix, 1986; Knoll, 2010).

As shown in Fig. 6, gold exhibits the highest stopping power across the investigated energy range, while hafnium oxide and iron oxide show progressively slightly lower values. In the low-energy region (1-15 MeV), corresponding to the proton energies simulated in this study, electronic stopping dominates, and material-dependent differences are most pronounced for gold. The higher stopping power of gold results in enhanced local energy transfer and increased production of secondary electrons near the nanoparticles. The observed hierarchy (Au $>$ HfO_2 $\approx$ Fe_2O_3) aligns with the DER trends obtained in this work, providing a robust physical explanation for the superior dose enhancement associated with gold nanoparticles.

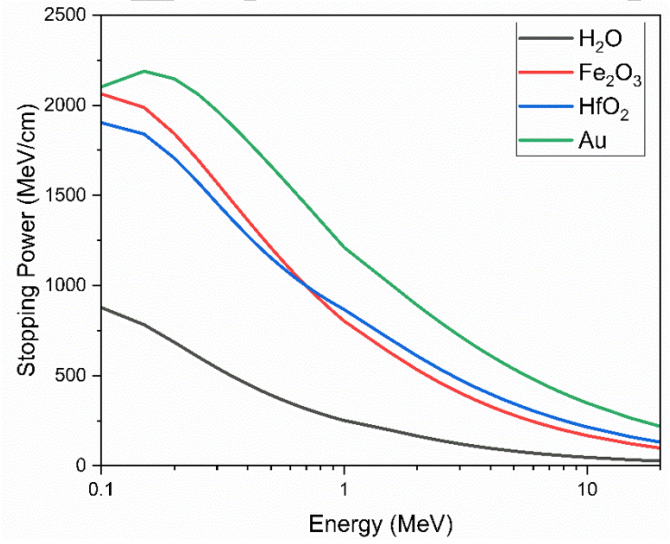

Figure 6: Proton stopping power in water, Au, HfO_2, and Fe_2O_3.

A critical interpretation of these modest DER values must first acknowledge the inherent limitation of the macroscopic dose enhancement ratio (DER) as the sole metric for evaluating nanoparticle efficacy. The DER, as calculated in this and similar Monte Carlo studies, quantifies the average increase in absorbed dose within a macroscopic volume (e.g., the cell nucleus or cytoplasm). While it accurately captures the contribution from proton slowing and the generation of secondary electrons via ionization, this macroscopic average inherently homogenizes and thus underestimates the highly localized and potentially biologically more effective energy deposition occurring at the nanoscale, immediately surrounding each nanoparticle. Phenomena such as localized increases in LET, elevated concentration of radical species, and nanoscale dose clustering -effects that have been implicated in the therapeutic enhancement observed in experimental studies (**?**Behrouzkia et al., 2019) are not resolved by the DER metric. Therefore, the modest macroscopic DER reported here does not preclude significant radiobiological enhancement at the cellular level.

A systematic comparison was performed in this study to establish a controlled benchmark for evaluating nanoparticle-enhanced proton therapy. While absolute DER values in our simplified single-cell model remained modest -peaking at approximately 1.8% for 15 MeV protons at 90 $\mathrm{mg.ml^{-1}}$- this is consistent with several prior Monte Carlo simulation studies (Rudek et al., 2019; Cunningham et al., 2021). Therefore, the present work establishes a robust controlled benchmark under identical simulation conditions, providing a clear parametric ranking of nanoparticle efficacy (Au $>$ HfO_2 $\approx$ Fe_2O_3) and identifying optimal parameters such as small diameter (5 nm) and high concentration (90 $\mathrm{mg.ml^{-1}}$). This systematic approach offers valuable guidance for the design of future experimental and clinical translation studies.

It is important to acknowledge the limitations of this computational study. A direct radiobiological assessment -such as quantifying DNA damage or cell survival- was beyond its scope, as these endpoints depend on complex biological responses not captured by physical dose deposition alone. This focus on physical dose is consistent with prior simulation work, which has indicated that the increase in direct DNA damage from the physical dose enhancement of gold nanoparticles in proton therapy may be negligible (Sotiropoulos et al., 2017). This finding further underscores the central argument of the present discussion: the macroscopic DER is an incomplete predictor of biological outcome. The potential for significant biological enhancement likely resides in the non-linear and spatially concentrated effects at the nanoscale (e.g., clustered damage, radical concentration) that are not resolved by the DER metric, reinforcing the need for the integrated multi-scale research trajectory outlined below.

5 Conclusions

In this GEANT4-based simulation study, the effects of various nanoparticle parameters on cellular dose enhancement (in both the cytoplasm and nucleus) under proton

irradiation were systematically investigated. The findings indicate that the incorporation of nanoparticles can increase the dose received by cells; however, the extent of this enhancement strongly depends on the nanoparticle material, concentration, and size. Among the nanoparticles examined, gold exhibited the most pronounced dose-enhancing effect, which can be attributed to its higher atomic number and density. Although the absolute dose enhancement values were relatively small at clinically relevant concentrations, the results provide valuable insights for optimizing treatment parameters to maximize the therapeutic efficacy of proton therapy.

Compared to our previous MCNP-based study (Bidokhti et al., 2025), the use of GEANT4 together with the GEANT4-DNA extension in the present work allowed for a more detailed track-structure description of proton interactions at nanometric scales. The ability of GEANT4-DNA to model the physical, physio-chemical, and chemical stages of energy deposition enabled a more realistic representation of secondary electron production around nanoparticles, thereby improving the accuracy of nanoscale dose predictions.

Furthermore, these findings suggest that careful selection of nanoparticle properties could allow for targeted dose escalation within tumor cells while minimizing effects on surrounding healthy tissue. To build upon this work, future studies should incorporate radiobiological assessments, such as DNA damage evaluation and cell survival assays, as well as experimental validation to confirm the simulation predictions. Overall, this study highlights the potential of nanoparticle-assisted proton therapy as a promising strategy for improving treatment outcomes in hadron therapy.

Acknowledgements

We sincerely acknowledge the High-Performance Computing Center of the University of Birjand for providing the computational infrastructure and their valuable support in conducting the Monte Carlobased simulations.

Conflict of Interest

The authors declare no potential conflict of interest regarding the publication of this work.

Funding

The authors declare that no funds, grants, or other financial support were received during the preparation of this manuscript.

References

Akhdar, H., Alanazi, R., Alanazi, N., et al. (2022). Secondary electrons in gold nanoparticle clusters and their role in therapeutic ratio: the outcome of a Monte Carlo simulation study. *Molecules*, 27(16):5290.

Alamgir, J., Hosseini, S., and Salimi, E. (2024). The simulation of dose variation effects due to the presence of different metal nanoparticles under proton irradiation using Geant4 toolkit. *Journal of Nuclear Science, Engineering and Technology (JONSAT)*, 45(2):54–64.

Alamgir, J., Hosseini, S. A., and Salimi, E. (2025). A Monte Carlo study on the impact of a transverse magnetic field on microscopic dose enhancement of nanoparticles in therapeutic proton beams. *Radiation and Environmental Biophysics*, 64(4):697–710.

Allison, J., Amako, K., Apostolakis, J., et al. (2016). Recent developments in Geant4. *Nuclear Instruments and Methods in Physics Research Section A: Accelerators, Spectrometers, Detectors and Associated Equipment*, 835:186–225.

Attix, F. H. (1986). *Introduction to radiological physics and radiation dosimetry*. Wiley, New York.

Behrouzkia, Z., Zohdiaghdam, R., Khalkhali, H., et al. (2019). Evaluation of gold nanoparticle size effect on dose enhancement factor in megavoltage beam radiotherapy using MAGICA polymer gel dosimeter. *Journal of Biomedical Physics & Engineering*, 9(1):89.

Bidokhti, P., Karimi-Shahri, K., and Ghorbani, G. (2025). Investigation of the effect of nanoparticle physical parameters on the efficiency of proton therapy for brain tumors using Monte Carlo simulation. *Journal of Torbat Heydariyeh University of Medical Sciences*.

Cao, Y., Zhou, X., Nie, Q., et al. (2024). Inhibition of the thioredoxin system for radiosensitization therapy of cancer. *European Journal of Medicinal Chemistry*, 268:116218.

Carbone, G. G., Mariano, S., Gabriele, A., et al. (2025). Exploring the potential of gold nanoparticles in proton therapy: Mechanisms, advances, and clinical horizons. *Pharmaceutics*, 17:176.

Chen, Y., Yang, J., Fu, S., et al. (2020). Gold nanoparticles as radiosensitizers in cancer radiotherapy. *International Journal of Nanomedicine*, pages 9407–9430.

Cunningham, C., de Kock, M., Engelbrecht, M., et al. (2021). Radiosensitization effect of gold nanoparticles in proton therapy. *Frontiers in Public Health*, 9:699822.

Gerken, L. R., Gogos, A., Starsich, F. H., et al. (2022). Catalytic activity imperative for nanoparticle dose enhancement in photon and proton therapy. *Nature Communications*, 13(1):3248.

He, M., Chen, S., Yu, H., et al. (2025). Advances in nanoparticle-based radiotherapy for cancer treatment. *iScience*, 28(1).

Incerti, S., Baldacchino, G., Bernal, M., et al. (2010). The Geant4-DNA project. *International Journal of Modeling, Simulation, and Scientific Computing*, 1(02):157–178.

Khan, F. M. and Gibbons, J. P. (2014). *The Physics of Radiation Therapy*. Lippincott Williams & Wilkins, Philadelphia, PA, 5th edition.

Knoll, G. F. (2010). *Radiation Detection and Measurement*. John Wiley & Sons, Hoboken, NJ, 4th edition.

Kwon, J., Sutherland, K., Hashimoto, T., et al. (2016). Spatial distributions of dose enhancement around a gold nanoparticle at several depths of proton Bragg peak. *Nuclear Instruments and Methods in Physics Research Section B: Beam Interactions with Materials and Atoms*, 384:113–120.

Kyriakou, I., Sakata, D., Tran, H. N., et al. (2021). Review of the Geant4-DNA simulation toolkit for radiobiological applications at the cellular and DNA level. *Cancers*, 14(1):35.

Lin, Y., Paganetti, H., McMahon, S. J., et al. (2015). Gold nanoparticle induced vasculature damage in radiotherapy: Comparing protons, megavoltage photons, and kilovoltage photons. *Medical Physics*, 42(10):5890–5902.

Liu, Y., Liu, X., Jin, X., et al. (2015). The dependence of radiation enhancement effect on the concentration of gold nanoparticles exposed to low- and high-LET radiations. *Physica Medica*, 31(3):210–218.

Ma, J., Shen, H., and Mi, Z. (2024). Enhancing proton therapy efficacy through nanoparticle-mediated radiosensitization. *Cells*, 13(22):1841.

Mansouri, E., Almisned, G., Tekin, H., et al. (2024). Radiosensitization with metallic nanoparticles under mev proton beams: local dose enhancement. *Radiation and Environmental Biophysics*, 63(4):537–543.

Martínez-Rovira, I. and Prezado, Y. (2015). Evaluation of the local dose enhancement in the combination of proton therapy and nanoparticles. *Medical Physics*, 42(11):6703–6710.

Mohan, R. (2022). A review of proton therapy–current status and future directions. *Precision Radiation Oncology*, 6(2):164–176.

Mohseni, M., Kazemzadeh, A., Ataei, N., et al. (2020). Study on the dose enhancement of gold nanoparticles when exposed to clinical electron, proton, and alpha particle beams by means of Geant4. *Journal of Medical Signals & Sensors*, 10(4):286–294.

Peukert, D., Kempson, I., Douglass, M., et al. (2020). Gold nanoparticle enhanced proton therapy: A Monte Carlo simulation of the effects of proton energy, nanoparticle size, coating material, and coating thickness on dose and radiolysis yield. *Medical Physics*, 47(2):651–661.

Polopetrakis, I., Kyriakou, I., Sakata, D., et al. (2025). New Geant4-DNA physics model for electron track-structure simulations in gold nanoparticles. *Physics in Medicine & Biology*, 70(16):165019.

Rajabpour, S., Saberi, H., Rasouli, J., et al. (2022). Comparing Geant4 physics models for proton-induced dose deposition and radiolysis enhancement from a gold nanoparticle. *Scientific Reports*, 12(1):1779.

Ramaekers, B. L., Pijls-Johannesma, M., Joore, M. A., et al. (2011). Systematic review and meta-analysis of radiotherapy in various head and neck cancers: comparing photons, carbon-ions and protons. *Cancer Treatment Reviews*, 37(3):185–201.

Rashid, R. A., Sisin, N. N. T., Razak, K. A., et al. (2025). Cell survival analysis of radiosensitization effects by gold nanoparticles for proton beam therapy. *Journal of Radiation Research and Applied Sciences*, 18:101203.

Rudek, B., McNamara, A., Ramos-Méndez, J., et al. (2019). Radio-enhancement by gold nanoparticles and their impact on water radiolysis for x-ray, proton and carbon-ion beams. *Physics in Medicine & Biology*, 64(17):175005.

Sah, B. and Antosh, M. P. (2019). Effect of size on gold nanoparticles in radiation therapy: Uptake and survival effects. *J. Nano Med*, 2:1013.

Shrestha, S., Cooper, L. N., Andreev, O. A., et al. (2016). Gold nanoparticles for radiation enhancement in vivo. *Jacobs Journal of Radiation Oncology*, 3(1):026.

Sotiropoulos, M., Taylor, M., Henthorn, N., et al. (2017). Geant4 interaction model comparison for dose deposition from gold nanoparticles under proton irradiation. *Biomedical Physics & Engineering Express*, 3(2):025025.

Tabbakh, F. (2024). Significance of the proton energy loss mechanism to gold nanoparticles in proton therapy: a Geant4 simulation. *Scientific Reports*, 14(1):24978.

Taheri, A., Khandaker, M. U., Moradi, F., et al. (2023). A review of recent advances in the modeling of nanoparticle radiosensitization with the Geant4-DNA toolkit. *Radiation Physics and Chemistry*, 212:111146.

Taheri, A., Khandaker, M. U., Moradi, F., et al. (2024). A simulation study on the radiosensitization properties of gold nanorods. *Physics in Medicine and Biology*, 69:045029.

Tsiamas, P., Liu, B., Cifter, F., et al. (2013). Impact of beam quality on megavoltage radiotherapy treatment techniques utilizing gold nanoparticles for dose enhancement. *Physics in Medicine & Biology*, 58(3):451.

Ziegler, J. F., Ziegler, M. D., and Biersack, J. P. (2010). SRIM The stopping and range of ions in matter (2010). *Nuclear Instruments and Methods in Physics Research Section B: Beam Interactions with Materials and Atoms*, 268(11–12):1818–1823.

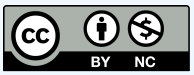

To cite this article:

P. Bidokhti, K. Karimi-Shahri, M. Ghorbani. Monte Carlo-based numerical assessment of metal and metal oxide nanoparticle parameters on cellular dose enhancement in proton therapy. *Radiation Physics and Engineering*, In Press.

DOI:

To link to this article: